



# Projections of heat waves with high impact on human health in Europe



A. Amengual<sup>a,\*</sup>, V. Homar<sup>a</sup>, R. Romero<sup>a</sup>, H.E. Brooks<sup>b</sup>, C. Ramis<sup>a</sup>, M. Gordaliza<sup>c</sup>, S. Alonso<sup>a,d</sup>

<sup>a</sup> Grup de Meteorologia, Departament de Física, Universitat de les Illes Balears, Palma, Mallorca, Spain

<sup>b</sup> NOAA/National Severe Storms Laboratory, Norman, OK, USA

<sup>c</sup> Facultad de Farmacia, Instituto de Estudios de la Ciencia y la Tecnología, Universidad de Salamanca, Salamanca, Spain

<sup>d</sup> Departament de Recerca en Canvi Global, Institut Mediterrani d'Estudis Avançats, Palma, Mallorca, Spain

## ARTICLE INFO

### Article history:

Received 9 January 2014

Received in revised form 21 May 2014

Accepted 26 May 2014

Available online 2 June 2014

### Keywords:

Climate change

Heat waves

Human health

Physiologically equivalent temperature

Regional climate modeling

Statistical adjustment

Ensemble strategy

## ABSTRACT

Climate change will result in more intense, more frequent and longer lasting heat waves. The most hazardous conditions emerge when extreme daytime temperatures combine with warm night-time temperatures, high humidities and light winds for several consecutive days. Here, we assess present and future heat wave impacts on human health in Europe. Present daily physiologically equivalent temperatures (PET) are derived from the ERA-Interim reanalysis. PET allows to specifically focus on heat-related risks on humans. Regarding projections, a suite of high-resolution regional climate models – run under SRES A1B scenario – has been used. A quantile–quantile adjustment is applied to the daily simulated PET to correct biases in individual model climatologies and a multimodel ensemble strategy is adopted to encompass model errors. Two types of heat waves differently impacting human health – strong and extreme stress – are defined according to specified thresholds of thermal stress and duration. Heat wave number, frequency, duration and amplitude are derived for each type. Results reveal relatively strong correlations between the spatial distribution of strong and extreme heat wave amplitudes and mortality excess for the 2003 European summer. Projections suggest a steady increase and a northward extent of heat wave attributes in Europe. Strong stress heat wave frequencies could increase more than 40 days, lasting over 20 days more by 2075–2094. Amplitudes might augment up to 7 °C per heat wave day. Important increases in extreme stress heat wave attributes are also expected: up to 40 days in frequency, 30 days in duration and 4 °C in amplitude. We believe that with this information at hand policy makers and stakeholders on vulnerable populations to heat stress can respond more effectively to the future challenges imposed by climate warming.

© 2014 Elsevier B.V. All rights reserved.

## 1. Introduction

Climate change is one of the major social, economic and environmental concerns of the twenty-first century. Observations show that global mean air surface temperature has notably increased during the last century (IPCC, 2007). Europe emerges as an especially responsive area to temperature rise, particularly during the warm season (Giorgi, 2004). European warming is projected to continue at a rate somewhat greater than the global mean (IPCC, 2007). Furthermore, projections indicate that heat waves will become more intense, more frequent and longer lasting (Meehl and Tebaldi, 2004). Together with a general mean warming over Europe, changes in temperature variability could exacerbate heat waves: even small increases in temperature variability could produce significant changes in heat wave attributes as a consequence of its threshold-based definition (Schär et al., 2004; Beniston et al., 2007; Kjellström et al., 2007; Fischer and Schär, 2009).

Population is highly vulnerable to changes in heat wave attributes. These may lead to increased mortality, mainly among the elderly, children and people with pre-existing health risks (Basau and Samet, 2002; Koppe et al., 2004). The 2003 European summer heat wave exemplifies possible social impacts, with a death toll exceeding 70,000 (Robine et al., 2008). Some studies have analyzed the link among climatic factors and mortality excess under heat wave conditions. For instance, heat-related mortality has been studied through a combination of extreme high daytime and over-night temperatures (Changnon et al., 1996; Trigo et al., 2009). By using the daily maximum apparent temperature (AT), Fischer and Schär (2010) projected the severest heat wave impacts on human health in southern Europe and the Mediterranean. After linking AT and mortality, Ballester et al. (2011) projected an increase in heat-related death toll for Europe, and suggested a shift in seasonality of maximum monthly mortality from winter to summer. But the thermal environment for humans encompasses both the thermal stress – i.e. the atmospheric heat exchanges with the body – and the thermal strain – i.e. the body's physiological response – (Jendritzky and Tinz, 2009).

Besides maximum and minimum temperatures and saturation deficit, other atmospheric variables also have an important role on

\* Corresponding author at: Dept. de Física, Universitat de les Illes Balears, 07122 Palma, Mallorca, Spain.

E-mail address: [arnau.amengual@uib.es](mailto:arnau.amengual@uib.es) (A. Amengual).

human thermal comfort. Wind speed, solar heat load and radiation exchange fluxes should be considered to assess as accurately as possible heat stress impacts under heat wave conditions. Furthermore, thermo-physiological parameters are a key factor to determine thermal stress impacts on human health. The human body balances heat production – and additional environmental heat gains – with heat loss. Heat production is a result of the metabolic activity required to perform mental and physical activities. Most of the energy that the body uses is released to the environment as heat through convection, conduction, radiation, respiration and evaporation (Koppe et al., 2004). Under heat wave conditions, heat loss is severely reduced and heat production can eventually exceed environmental losses. When internal mechanisms regulating body temperature are stressed and cannot cope with thermo-regulatory demands, the body temperature increases. This can lead to excessive strain on the body and ultimately cause heat illness and an increase on heat-related excess mortality and morbidity.

We study heat wave impacts on human health in Europe by using the physiologically equivalent temperature (PET). PET is a thermal index based on a complete heat budget of the human body and encompasses both meteorological and thermo-physiological aspects (Mayer and Höppe, 1987; Höppe, 1999; Matzarakis et al., 1999). PET has already been used to assess the relationship between heat stress and mortality in Europe. Matzarakis et al. (2011) found a significant impact of heat stress on human health after evaluating a 37-year period of daily data in the federal state of Vienna, Austria. In particular, an enhanced risk of mortality to heat stress was found due to cardiovascular and respiratory diseases. Matzarakis and Nastos (2011) analyzed heat wave impacts on humans for the Greater Athens Area during the 1955–2001 period. Impacts on human health were described through the intensity and duration of the heat waves by using daily physiologically equivalent and minimum air temperatures. An increase in the average duration of heat waves was found for this period. These authors also revealed the relevance for humans of the intra-annual variation of heat stress conditions. The association between daily mortality and thermal conditions has also been recently examined by Nastos and Matzarakis (2012) for Athens, Greece. After analyzing 10-year daily series of minimum and maximum temperatures and the PET and Universal Thermal Climate (UTCI; see special issue of Int. J. Biometeorol. 56, 2012) indices, mortality was found closely related to all these parameters. In addition, the authors showed strong statistical relationships between mortality and air temperatures, PET and UTCI on the same day. Thus, we first derive daily PETs from the ECMWF ERA-Interim reanalysis. Next, we define strong and extreme stress heat waves by combining different daily maximum and minimum PET and duration thresholds. This allows to analyze the spatial distribution of European heat wave attributes for the current climate.

Regarding future scenarios, reliable projections of climatic variables from Regional Climate Models (RCMs) are required to properly assess regional and local impacts. Such evaluation is made by driving impact models with RCM outputs. However, it would be advisable to previously

**Table 1**

Physiological equivalent temperature ranges, in °C, for different grades of thermal stress.

Adapted from Matzarakis and Mayer (1997).

Thermo-physiological stress	PET thresholds
Extreme cold stress	<4
Strong cold stress	4–8
Moderate cold stress	8–13
Slight cold stress	13–18
No thermal stress	18–23
Slight heat load	23–29
Moderate heat load	29–35
Strong heat load	35–41
Extreme heat load	>41

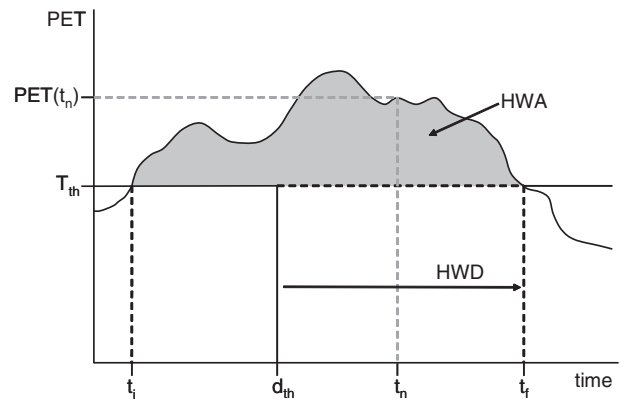


**Fig. 1.** Graphical sketch of heat wave duration (HWD) and amplitude (HWA, gray shading) exceedances.  $T_{th}$  and  $d_{th}$  denote the thermal stress and duration thresholds, respectively.

calibrate the simulated variables – or their derivatives – in order to correct model biases, rather than to drive impact models with raw RCM outputs. Systematic discrepancies occur between simulated and observed climate. Model errors arise from inaccuracies in the physical and sub-grid scale parametrizations and uncertainties in the boundary forcing. Among the different correction techniques, quantile–quantile mapping adjustments are one of the most suitable (Wood et al., 2004; Boé et al., 2007; Déqué, 2007; Amengual et al., 2012). Prior to examining future changes in heat wave attributes, we apply the quantile–quantile adjustment described in Amengual et al. (2012) to the daily PET cumulative distribution functions (CDFs) of each individual RCM. These RCMs were run under the SRES A1B scenario and by considering a diversity of RCMs and parent GCMs in a regional multimodel ensemble, we naturally account for and potentially smooth out model errors.

The structure of the paper is as follows: Section 2 introduces the physiologically equivalent temperature and provides a definition of heat waves; Section 3 describes the observed and simulated databases, the thermal sensation derivation and the quantile–quantile adjustment; Section 4 evaluates the link between heat waves and mortality excess for the 2003 European summer and describes present and projected changes in heat wave attributes; finally, Section 5 summarizes the main results and conclusions, offering some additional remarks.

## 2. Definitions

### 2.1. Physiologically equivalent temperature

Energy balance models of the human body take all mechanisms of heat exchange into account, being thermo-physiologically relevant to

**Table 2**

List of transient RCM experiments driven within the ENSEMBLES European project for the 1951–2100 period. Note that all models have a spatial resolution of 25 km and were run under the SRES A1B.

Driving GCM	RCM	Acronym	Institute
ECHAM5	RCA3	C4IRCA3	C4I
ARPEGE	HIRLAM	DMI-HIRLAM5	DMI
ECHAM5	HIRLAM	DMI-HIRLAM5	DMI
BCM	HIRLAM	DMI-HIRLAM5	DMI
HadCM3	CLM	ETHZ-CLM	ETHZ
ECHAM5	RegCM	ICTP-REGCM	ICTP
ECHAM5	RACMO	KNMI-RACMO	KNMI
HadCM3	HadRM3Q0	METO-HC-HadCM3Q0	HC
HadCM3	HadRM3Q3	METO-HC-HadCM3Q3	HC
HadCM3	HadRM3Q16	METO-HC-HadCM3Q16	HC
BCM	RCA	SMIRCA	SMHI
ECHAM5	RCA	SMIRCA	SMHI
HadCM3	RCA	SMIRCA	SMHI

individual exposures and experiences (Koppe et al., 2004; Blazejczyk et al., 2012). Thermal stress indices derived from these models are known as rational indices. Among these, the physiologically equivalent temperature is based on a complete heat budget model (Mayer and Höppe, 1987; Höppe, 1999). PET provides the equivalent air temperature of a reference indoor environment with a water vapor pressure of 12 hPa (approximately equivalent to 50% of relative humidity at 20 °C) and light wind ( $0.1 \text{ ms}^{-1}$ ), at which the heat balance of a standardized person is maintained with core and skin temperatures equal to that under the conditions being assessed. Influence of air temperature on PET is accounted for through the convective heat flow and the heat flows used for heating and humidifying the inspired air. The influence of the water vapor gradient is restricted to latent heat exchange fluxes via respiration and diffusion (i.e., imperceptible perspiration) through the skin. Latent heat fluxes via evaporation of sweat are excluded. Wind speed effects are considered by means of heat loss by convection and evaporation. The net radiation of the body is taken into account via the mean radiant temperature of the surroundings ( $T_{mrt}$ ). Thermophysiological parameters are considered through human activity – which is added to a reference metabolic heat – and cloth isolation (Höppe, 1999; Matzarakis et al., 1999). Thus, the dominant meteorological parameters influencing the human energy balance are: air temperature, saturation pressure deficit, wind velocity and mean radiant temperature. The PET assessment scale (Table 1) is derived by calculating the predicted mean vote (PMV; Fanger, 1972; Fanger et al., 1974) for varying air temperatures in the reference environment using the setting for the reference person (Matzarakis and Mayer, 1997). Hence, PET is a comfort based thermal index.

## 2.2. Heat wave

There is no standard definition for a heat wave. These are rare events that vary in character and impact even in the same location. Although the World Meteorological Organization (WMO) has not yet defined the term, several approaches can be used to define a heat wave (Koppe et al., 2004; Meehl and Tebaldi, 2004). These are usually defined from absolute or relative thresholds – or as a combination of both – of weather variables. The adoption of absolute parametric thresholds guarantees the rigorous analysis of extreme events of a fixed intensity as opposed to the use of relative thresholds which measure extreme episodes of a fixed rarity (Beniston et al., 2007).

When using daily maximum temperatures – or even thermal indices combining the effect on humans of several meteorological variables

(e.g. heat index, effective temperature or apparent temperature), relative thresholds are more commonly used, having the advantage of accounting for both local differences in climatology (e.g. Beniston et al., 2007; Fischer and Schär, 2010). On the other hand, thermal stress indices derived from heat budget models for humans are used as physiological standards to assess occupational environment (Blazejczyk et al., 2012). These indices rely on the heat balance equation and encompass more absolute or fixed aspects of human physiology, since thermophysiological functions are fundamentally the same among populations. Thus, standard physiological indices are more commonly used by applying absolute thresholds (e.g. Matzarakis and Amelung, 2008; Jendritzky and Tinz, 2009; Muthers et al., 2010; Bröde et al., 2012; Nastos and Matzarakis, 2012). As we are using the physiologically equivalent temperature in this study, we define heat waves based on absolute thresholds in order to assess heat thermal stress for Europeans.

Two kinds of heat waves are defined depending on intensity. That is, by combining different PET (i.e. thermal stress,  $T_{th}$ ) and duration ( $d_{th}$ ) absolute thresholds:

- A *strong stress heat wave (SHW)* is a spell of at least  $d_{th} = 6$  consecutive days with daily maximum PETs exceeding a thermal sensation of  $T_{th}^{max} = 35 \text{ °C}$
- A *extreme stress heat wave (EHW)* is a spell lasting  $d_{th} = 3$  or more consecutive days with daily minimum and maximum PETs above  $T_{th}^{min} = 18 \text{ °C}$  and  $T_{th}^{max} = 41 \text{ °C}$ , respectively.

These PET thresholds are set from different grades of thermal perception and physiological stress on human beings to specifically address heat-related risks (Table 1). Daily maximum PETs greater than 35 °C imply a strong grade of physiological stress for Europeans (Matzarakis and Amelung, 2008). Furthermore, the most severe heat-related risks result from multi-day heat waves associated with warm nights. The latter strongly affect health by preventing the recovery from daytime heat stress and by aggravating the impact through sleep deprivation (Fischer and Schär, 2010). Thus, daily maximum PETs above 41 °C together with daily minimum PETs exceeding 18 °C imply an extreme grade of human physiological stress. The former threshold means utmost daytime heat stress, and the latter is the highest PET value at which humans do not suffer thermal stress (Matzarakis et al., 1999; Blazejczyk et al., 2012). Night-time physiologically equivalent temperatures higher than this value do not allow the human body to recover from the daytime extreme heat stress.

Regarding heat waves durations, these have been set according to previous research (e.g. Robinson, 2001; Beniston et al., 2007). Since

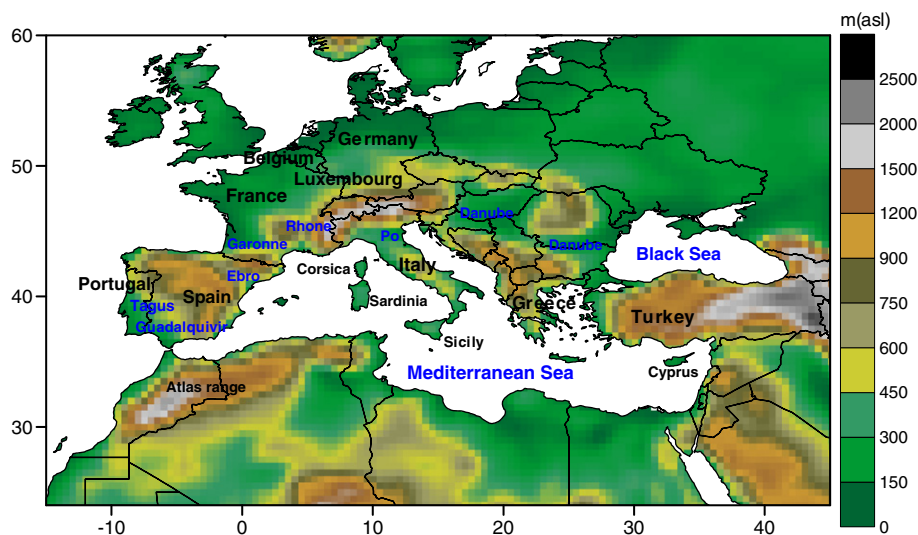


Fig. 2. ERA-Interim topography of the study domain. Geographic features mentioned in the text are indicated. Note that the geographical extent is determined by the smallest spatial domain among the considered RCMs.

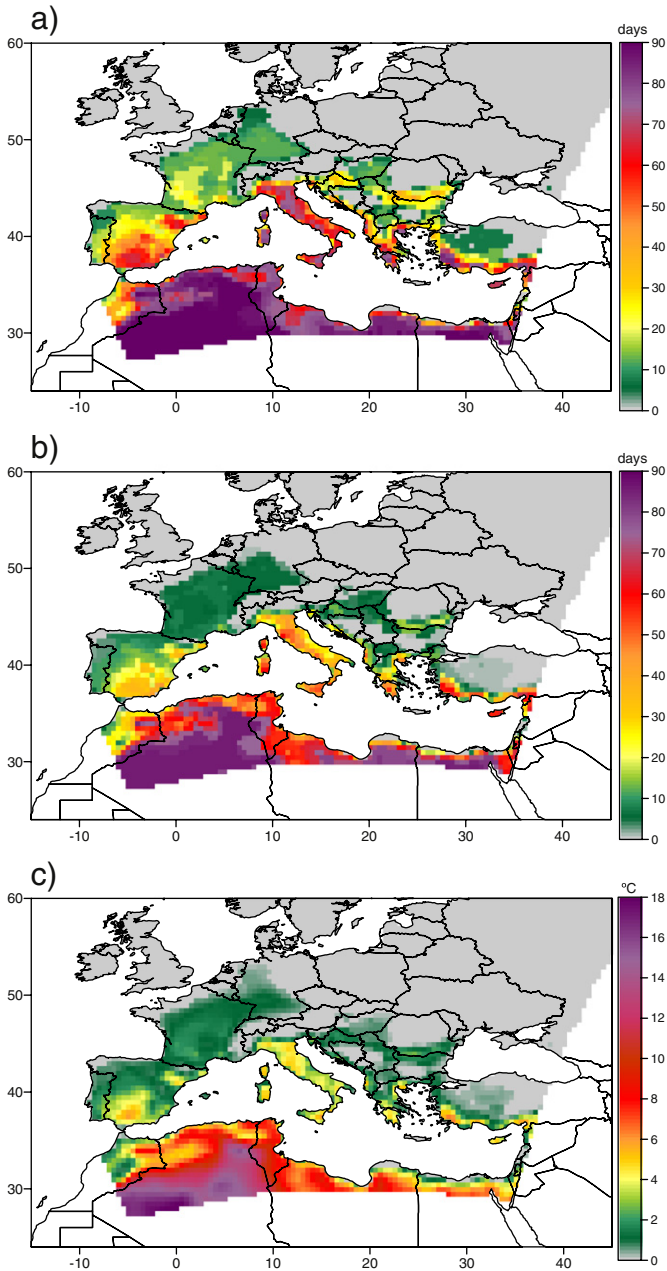


Fig. 3. SHW frequency (a), duration (b) and amplitude (c) for the summer of 2003.

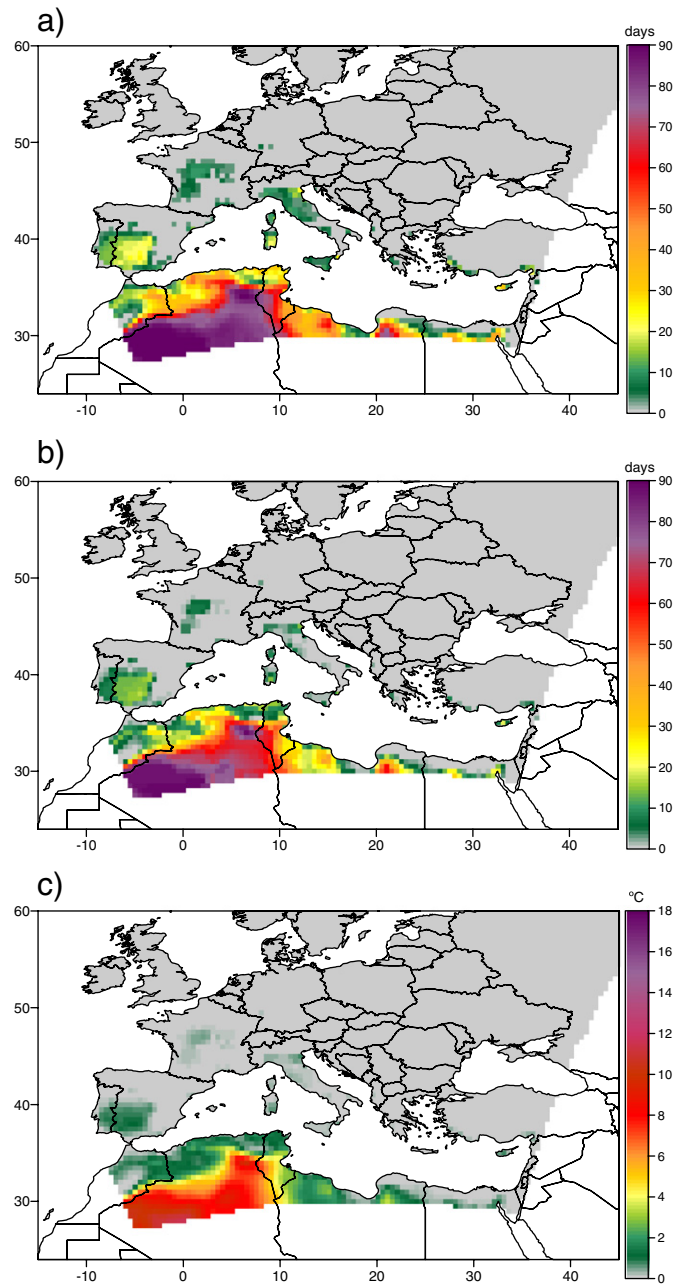


Fig. 4. As in Fig. 3, but for EHW.

short heat episodes can adversely affect human health, EHWs intend to encompass health problems related with a sudden and very intense increase in the environmental heat stress conditions. In fact, there is evidence that morbidity and mortality under heat wave conditions are more likely from the second warm night, when the interior of households without air conditioning are expected to reflect the outdoor thermal stress. SHWs intend to cope with the projected increase in the number of long heat waves in a warmer climate. Once SHW and EHW are defined, we characterize their attributes with the following parameters:

- *Heat wave number (HWN)*: the number of heat waves that occur in a given time interval (e.g. our baseline period)
- *Heat wave day frequency (HWF)*: the number of days under heat wave conditions in a given time interval

- *Heat wave duration exceedance (HWD)*: the total number of consecutive days exceeding the duration threshold for all heat waves in a given time interval. HWD accounts for the whole amount of excess days (Fig. 1). That is,

$$HWD = HWF - d_{th} \cdot HWN \quad (1)$$

- *Heat wave amplitude exceedance (HWA)*: the accumulated thermal stress exceedance for all the days under heat wave conditions in a given time interval (Fig. 1). HWA is expressed in degree-days and is specifically defined as:

$$HWA = HWT - T_{th} \cdot HWF \quad (2)$$

where HWT is the integral of the physiologically equivalent temperatures over the duration of each individual heat wave, and accumulated for all heat waves in a given time interval. That is,

$$HWT = \begin{cases} \sum_{HW_j} \int_{t_{ij}}^{t_{jf}} PET_{max}(t) dt & \text{and } T_{th} = T_{th_{max}} \text{ in (2) for SHW} \\ \sum_{HW_j} \int_{t_{ij}}^{t_{jf}} PET_{mean}(t) dt & \text{and } T_{th} = T_{th_{mean}} \text{ in (2) for EHW} \end{cases} \quad (3)$$

where  $t_{ij}$  and  $t_{jf}$  stand for the initial and the final time – the first and last day in our case – under the  $j$ -th heat wave conditions and  $T_{th_{mean}} = \frac{T_{th_{min}} + T_{th_{max}}}{2}$ .

### 3. Databases and methods

#### 3.1. Input data and thermal sensation derivation

The assessment of regional climate change impacts requires long-term atmospheric databases at high spatial and temporal resolutions. ECMWF ERA-Interim reanalysis has been adopted to represent the observed climate baseline in order to derive present physiologically equivalent temperatures. ERA-Interim currently covers a period starting from 1 January 1989 till present. Unlike ERA-40, ERA-Interim relies on the application of a four-dimensional variational analysis which uses observations every 12 h to initialize the forecast model, as well as on a better formulation of background error constraint, a new humidity analysis, an improved model physics, a variational bias correction of satellite radiance data and an improved fast radiative transfer model (Dee et al., 2011). The atmospheric model and reanalysis system is configured with 60 levels in the vertical, a grid spacing of 0.7°, 3-hourly surface and 6-hourly upper-air data output. Daily gridded data of 2 meter temperature, 2 meter dew-point temperature, total cloud cover and 10 meter wind speed have been obtained for the 1990–2009 period. The Bolton equation has been used to obtain relative humidity from temperature and dew-point depression (Bolton, 1980). Note that daily atmospheric variables have been retrieved from reanalysis at 00 and 12 UTC in order to derive as accurately as possible the minimum and maximum popularly sensible thermal sensations of each day.

For the projections, we have used the regional simulations available from the ENSEMBLES European project (Hewitt and Griggs, 2004). Climatic data from 13 different RCMs run from 1951 to 2100 for the A1B emission scenario have been considered (Table 2). Recall that SRES A1B is a moderate scenario being characterized by an emphasis not only on globalization and material wealth, but also on an equitable balance between the use of fossil and non-fossil fuels (Nakicenovic et al., 2000). The experiments were performed by using a grid spacing of 25 km that spans Europe and includes the easternmost part of the Atlantic ocean, northern Africa and western Asia (further information at <http://ensembles-eu.metoffice.com>). Daily analyzed and simulated atmospheric variables have been bilinearly interpolated from the four nearest grid-points of the ERA-Interim and individual model meshes to a common user-defined grid (Akima, 1978, 1996). This mesh covers Europe, Middle East and North Africa and has a spatial resolution of 0.5° × 0.5°, with a geographical extent being determined by the smallest spatial domain among the considered RCMs (Fig. 2).

Thermal conditions have been computed using the RayMan-Pro model (Matzarakis et al., 2007, 2010). RayMan-Pro accounts for the body-atmosphere energy budget schemes and derives PET from  $T_{mrt}$ . PET has been obtained by setting up the following daily meteorological parameters in RayMan-Pro: air temperature, relative humidity, wind speed and cloud cover. Then, water vapor pressure is derived from air

temperature and relative humidity. RayMan-Pro also includes the subsequent geographic and thermo-physiological parameters: longitude, latitude, local time, human activity, body heat production and heat transfer resistance of clothing. PET has been computed by considering the following standard personal and thermo-physiological parameters: height = 1.75 m; weight = 75 kg; age = 35 yr; sex = male; clothing = 0.9 clo and physical activity = 80 W (Matzarakis et al., 1999). Internal heat production and cloth isolation correspond to a reference person characterized by light activity (ASHRAE, 2004). Note that 1 clo = 0.155 km<sup>2</sup>W<sup>-1</sup>.

#### 3.2. Quantile–quantile adjustment approach

Reliable projections of climatic variables – and their derivatives – are required from RCMs to suitably assess climate change impacts. Since heat wave attributes have been derived from absolute PET thresholds, these are particularly sensitive to biases in model climatology (Fischer and Schär, 2010). Therefore, to properly use model outputs, it is first advisable to correct these errors. Even if dynamical downscaling improves the representation of regional features in climate projections, some important inaccuracies still remain owing to insufficient resolution of regional and local forcings, uncertainties in sub-grid scale parametrizations and model parameters. Corrections as the delta method or unbiasing procedures assume that the variability in the climate scenario remains unchanged or that model variability is perfect, respectively (Déqué, 2007; Ho et al., 2012). The application of quantile–quantile (Q–Q) mapping transformations is more flexible. These adjustments have been widely used for reducing errors in simulated climate variables (Reichle and Koster, 2004; Wood et al., 2004; Boé et al., 2007; Déqué, 2007).

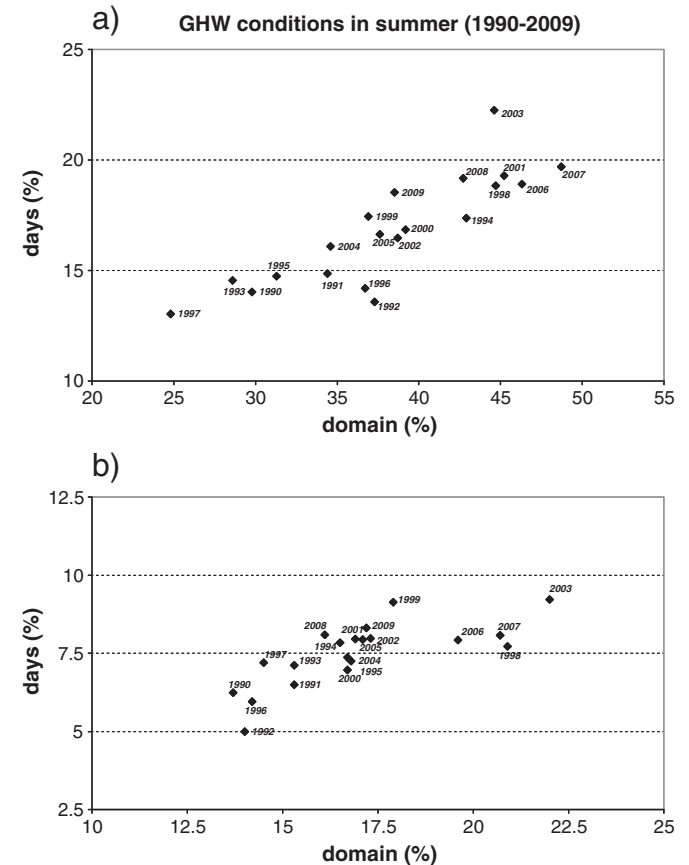


Fig. 5. Temporal and spatial coverage of (a) SHW and (b) EHW conditions for the 1990–2009 summers.

We apply the Q–Q adjustment described in detail in Amengual et al. (2012). Briefly, this approach accounts for discrepancies in model ability to reproduce the whole probability distribution function (PDF) of the observed atmospheric variables. Calibration is based on a non-parametric function that amends mean, variability and shape errors in the simulated cumulative distribution functions (CDFs). First, PETs are derived from daily data coming from ERA-Interim and each individual climate model. Then, the 20-year observed and simulated PET baselines, as well as successive future simulated intervals of the same length are considered in order to build their respective CDFs. Differences between future and baseline simulated CDFs are calculated quantile to quantile for the whole distributions. A basic correction approach would consist of simply adding these quantile differences to the observed baseline

CDF quantiles. However, the adjustment first splits these into two components: (i) the average difference between both distributions and, (ii) the perturbation of the quantile difference with respect to the average.

Next, each component is added to the observed CDF quantile with a weighting factor that depends on model error in order to obtain projected CDFs (Amengual et al., 2012). That is, changes between present and future daily simulated data are locally rescaled quantile by quantile on the basis of the observed CDF. The performance of the quantile–quantile adjustment was successfully tested by Amengual et al. (2012). They compared ensemble-mean calibrated and raw original distributions of several atmospheric variables against observed CDFs for an independent validation period. An overall improvement

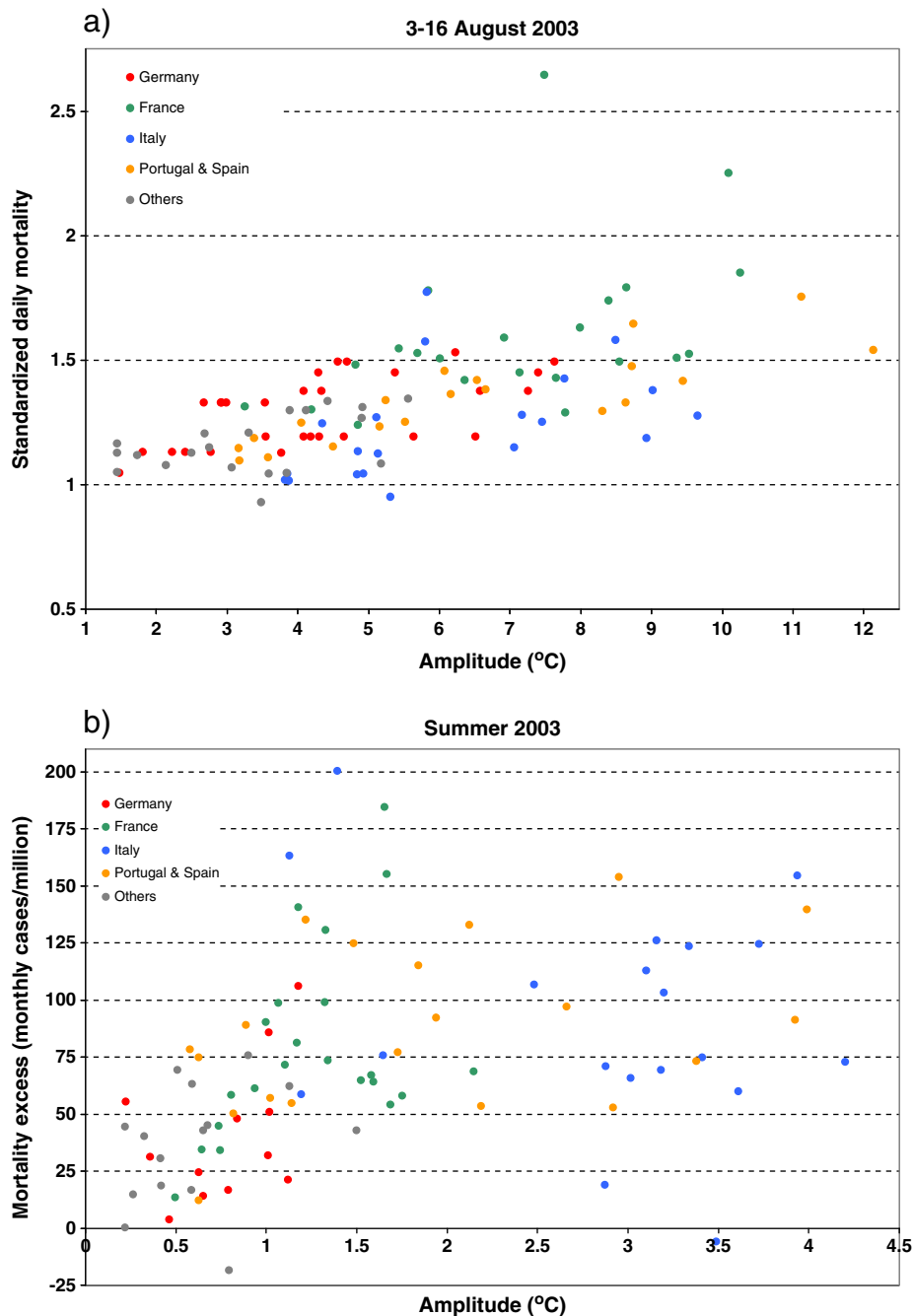


Fig. 6. Scatter plots of (a) the standardized daily death frequencies against SHW and EHW amplitudes from 3 to 16 August 2003; and (b) the monthly excess mortality against SHW and EHW amplitudes for the summer of 2003. Colored dots highlight regions of particular interest.



**Fig. 7.** The 111 NUTS2 regions – comprising 12 European countries – considered for the evaluation of the strong and extreme heat waves definitions. NUTS2 states for the second level of the Nomenclature of Territorial Units for Statistics in Europe.

was found in both the calibrated CDFs and climatological distributions of the atmospheric parameters. In addition, the spread among the models was adequately reduced: after amending possible biases and variability errors, RCMs are safely equiprobable.

#### 4. Results and discussion

##### 4.1. The 2003 European summer heat wave

We consider the 2003 European summer heat wave as a valuable prototype to examine the significance of our methods (i.e., definitions of heat wave attributes) and their relationship to heat-related mortality excess. Central and southwestern Europe were affected by a severe and persistent heat wave during the summer of 2003, and the economic and societal consequences were disastrous (Schär and Jendritzky, 2004). This extreme warm episode was produced by a semi-stationary 500-hPa positive geopotential height anomaly. These anomalies are associated with specific atmospheric circulation patterns that produce subsidence, clear skies, light winds, warm-air advection and prolonged hot conditions at surface. Projected 500-hPa height increases over the southern Europe and the Mediterranean will be directly associated with more severe heat waves in the future (Meehl and Tebaldi, 2004). The 2003 European summer heat wave raised temperatures by 3 to 5 °C above the 1961–90 average in most of southwestern and central Europe. In June, warm anomalies increase the monthly mean temperature up to 6–7 °C, July was only slightly warmer than average (about 1–3 °C), and the highest deviations were reached during the first half of August (+7 °C; Fink et al., 2004). Although mean summer

temperatures were far above the long-term mean values, these are consistent with a combined increase in mean temperature and temperature variability (Schär et al., 2004; Fischer and Schär, 2009). Death toll of heat-related mortality exceeded 70,000 in Europe: 11,000 in June, 10,000 in July, and 15,000 and 24,000 during the first and second weeks of August, respectively (Robine et al., 2008).

Figs. 3 and 4 show the spatial distributions of strong and extreme stress heat wave attributes during this record-breaking warm episode. Apart from North Africa, the highest SHW frequencies – above 70 days – are found in central Italy, Corsica, Sardinia, Sicily and in the southernmost parts of Greece and Turkey (Fig. 3a). Very high SHW frequencies – of 50–60 days – are also found in south, central and Mediterranean Spain and, to a lesser extent, in south and central France. High SHW frequencies are located in some of the most important river basins in southern Europe (i.e., the lower Tagus river in Portugal, the Guadalquivir and Ebro river basins in Spain, the Garonne and Rhone rivers in France, the Po river in Italy and the lower Danube river basin). Furthermore, Fig. 3 depicts a spell of SHW conditions over north and western France, south and western Germany, southwestern Belgium and Luxembourg, with frequencies up to 10–15 days. The maximum values of EHW attributes are found in the Tagus and Guadalquivir river basins (above 25 days for the frequency, Fig. 4a). EHW frequencies between 10 and 20 days occurred in southwestern and central France, in central and north Italy, Corsica, Sardinia and Sicily.

Fig. 5 shows persistence against areal extent for SHWs and EHWs in the 1990–2009 summers. Although the 2003 European heat wave exhibits the greatest number of days under strong stress conditions, the less severe 2006 and 2007 European heat waves had a larger spatial

**Table 3**

Correlation coefficients (R) and its confidence level (p) for standardized daily death frequencies against heat wave amplitudes for 3–16 August 2003. Also shown between brackets are the 95% correlation confidence intervals.

Heat wave intensity	R	p
SHW	0.62 (0.49, 0.72)	>99%
EHW	0.27 (−0.01, 0.51)	94%
HW	0.61 (0.47, 0.71)	>99%

**Table 4**

Correlation coefficients (R) and its confidence level (p) for monthly excess mortality against heat wave amplitudes for the summer of 2003. Also shown between brackets are the 95% correlation confidence intervals.

Heat wave intensity	R	p
SHW	0.38 (0.19, 0.55)	>99%
EHW	0.24 (−0.02, 0.48)	93%
HW	0.41 (0.22, 0.57)	>99%

extent (Fig. 5a). The former affected several northern and northwestern Europe countries in July 2006, and the latter large extents of southeastern Europe and the Balkans during the second half of June 2007. Furthermore, the 1998 and 2001 summers exhibit similar spatial coverage than the 2003 summer. The 2003 heat wave extent was not exceptional in terms of strong stress conditions, indicating that mortality excess for these circumstances would be more related to duration. For extreme heat wave conditions, the 2003 summer clearly exhibits the longest persistence and the largest extent, thus impacting European regions seldom affected by these kinds of heat waves (Fig. 5b). When considering SHW and EHW conditions together, the 2003 European heat wave lasted for more than 30% of the seasonal days and affected more than 65% of the entire study domain. Southwestern Europe was under a long lasting mix of strong and extreme stress conditions. Those European regions not so well adapted to high-impact heat waves suffered the most damaging consequences on human health.

#### 4.2. The 2003 European mortality excess and heat wave amplitudes

Rather than frequency or duration, amplitude is the most relevant attribute to evaluate social impacts of heat waves. HWA integrates the accumulated heat stress excess on humans over the entire period under heat wave conditions (Eqs. (2) and (3); Fig. 1). For the sake of a calibration reference, we evaluate strong and extreme HWAs against heat-related mortality excess data from 3 to 16 August 2003 and for the entire 2003 summer. Furthermore, we consider separately and jointly SHW and EHW amplitudes. By evaluating together both kinds of heat waves (i.e., summing up their amplitudes), we better encompass the 2003 European summer heat wave, which consisted of consecutive alternating SHW and EHW conditions during a long period. However, the relationship between critical accumulated thermal stress and

mortality excess is not straightforward. Even when using PET as a thermal standard index to better encompass heat wave impacts on health for Europeans, critical thresholds are strongly modulated by demographic factors (age or sex), health status (pre-existing health risks) and socio-economic aspects (building and household insulation and acclimatization; Basau and Samet, 2002; Koppe et al., 2004; Fischer and Schär, 2010; Ballester et al., 2011). Recall that PETs have been derived from standard personal and thermo-physiological values, thus accounting for mean population similarities rather than for inter-individual differences.

Fig. 6a depicts the scatter-plot of the standardized daily death excess frequencies – expressed as the differences between 3 to 16 August 2003 and the 1998–2002 summer baseline – against SHW and EHW amplitudes for 111 European NUTS2 regions (Fig. 7). Note that standardized daily death frequencies of 1 means equal to the median death toll for the 1998–2002 summer average whereas a value of 2 means twice the median death number (Robine et al., 2008). NUTS2 amplitudes are calculated as the mean value of all grid-point amplitudes lying within each region. Finally, NUTS2 amplitudes are normalized by the number of days of each considered period. The spatial correlation between both heat wave amplitudes and daily death excess frequencies from 3 to 16 August 2003 is of 0.61 (Table 3 and Fig. 6a). SHW amplitudes show a slightly higher positive correlation than EHW (Table 3, individual figures not shown). Nevertheless, a robust spatial evaluation is somehow more difficult for the latter, because fewer NUTS2 regions – 51 – were under extreme stress heat wave conditions. Even so, the probability of no correlation between mortality excess and extreme HWA is as low as 6% (Table 3).

Regarding the summer of 2003, mortality excess data is available for 88 European regions. As discussed in Ballester et al. (2011), some of these were merged from the original NUTS2 areas in order to avoid

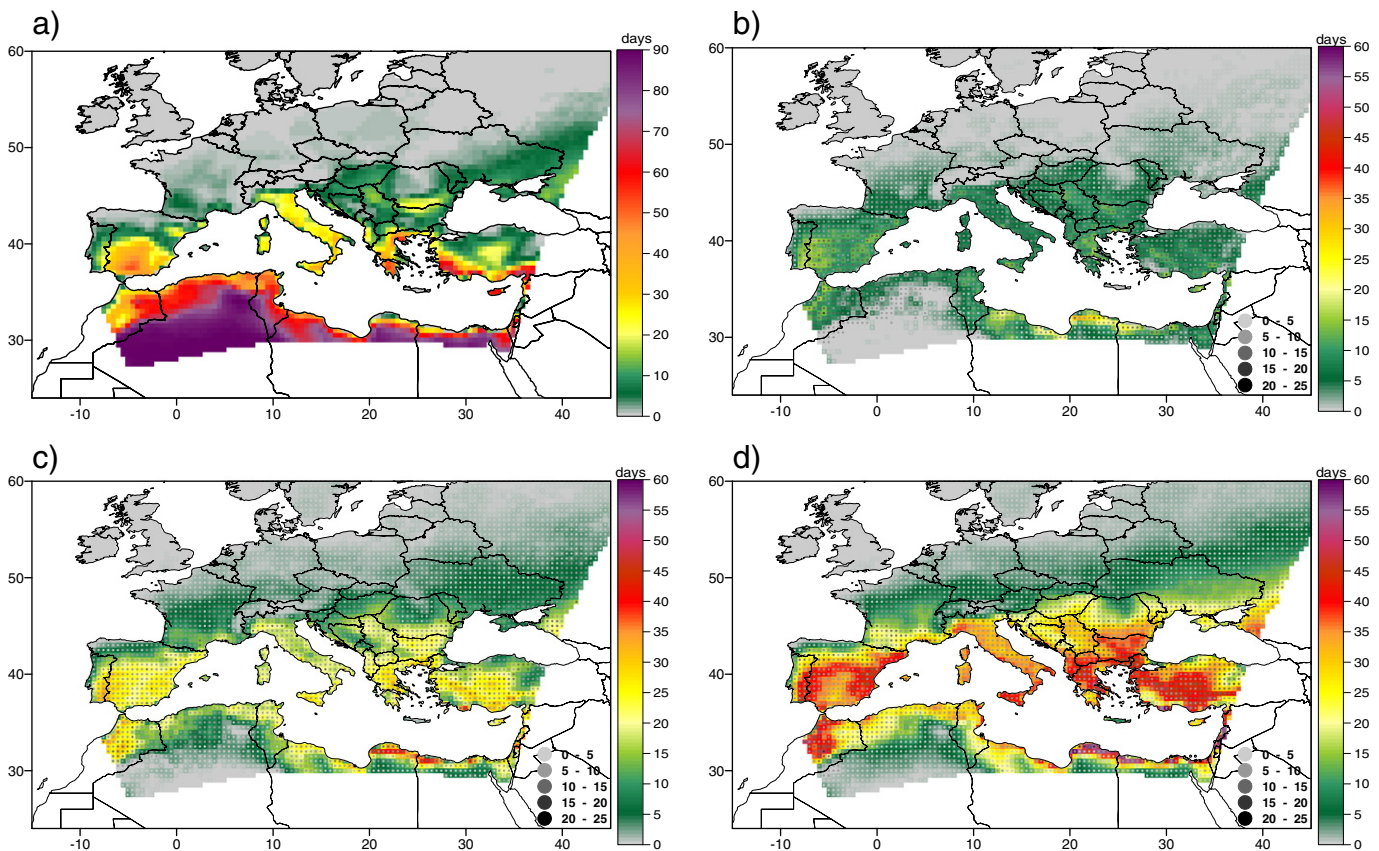


Fig. 8. Spatial distribution of (a) present (1990–2009) SHW frequencies in summer; and projected ensemble-mean absolute changes for (b) early (2015–34), (c) mid (2045–64) and (d) late (2075–94) twenty-first century. Shaded circles show the ensemble-standard deviation according to the scale. Absolute changes and standard deviations are expressed as number of days.

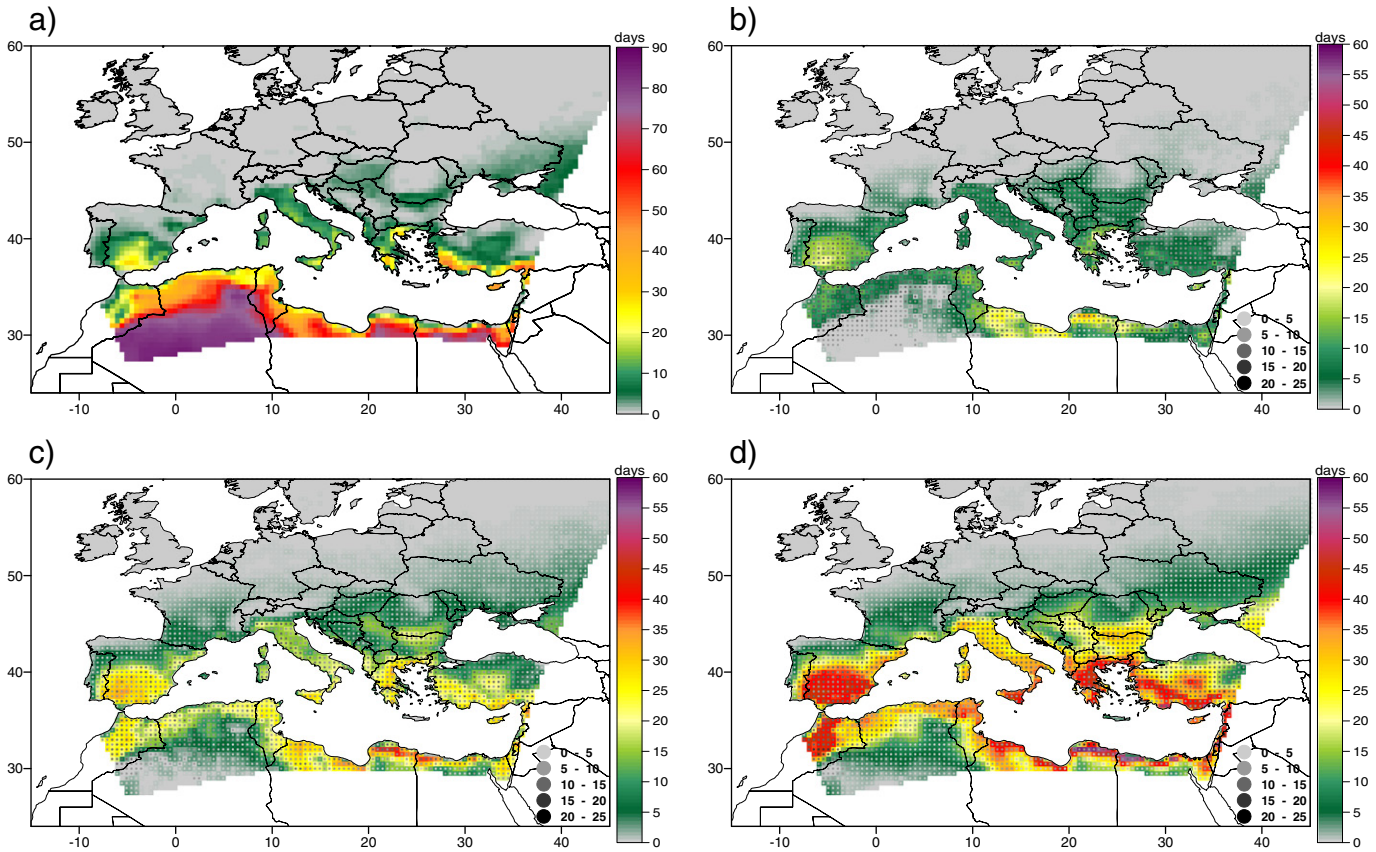


Fig. 9. As in Fig. 8, but for SHW durations.

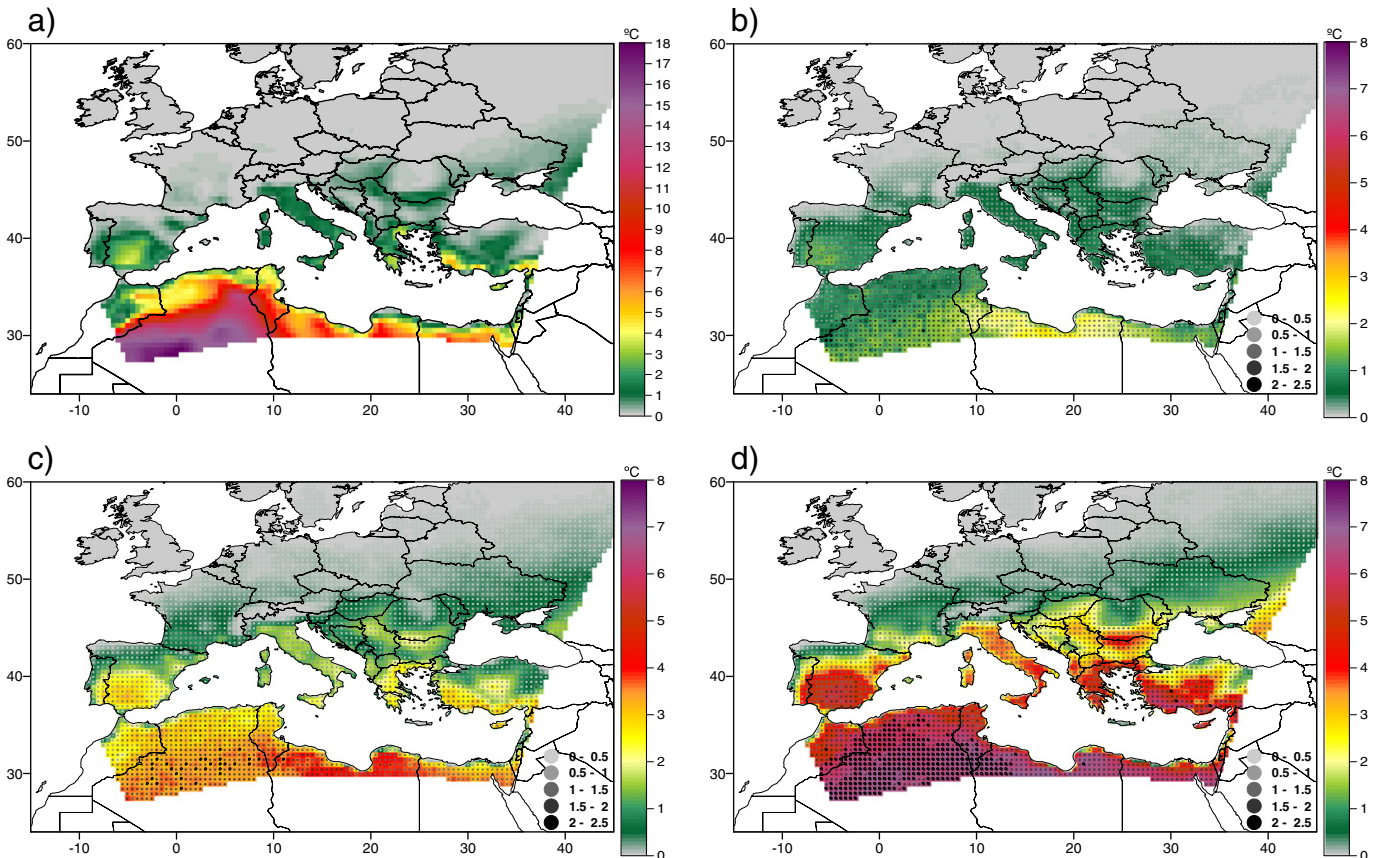


Fig. 10. As in Fig. 8, but for SHW amplitudes. Absolute changes and standard deviations are expressed as °C.

the biases introduced by large differences in population among them. Spatial anomalies were computed as the difference between the 2003 summer mortality and mean mortality for the 1998–2002 summers. A higher spread is found between SHW and EHW amplitudes and mortality excess for the entire 2003 summer. Thus, correlations are lower than for the first two weeks of August (Table 4). The highest correlation is found when combining the effects of SHW and EHW amplitudes (Fig. 6b). And, again, the lowest value is exhibited for EHW amplitudes, since few European regions – 55 – were affected by extreme conditions. In addition, EHWs are more spatially scattered than SHWs, being somehow more difficult to evaluate (Figs. 3 and 4). However, the significance level of these correlation values is very low and thus the attributed relationship between mortality excess and extreme HWA being spurious is unlikely (Table 4). In addition, weak regional differences among the European countries are devised for both periods. Since the 2003 heat wave shares a close resemblance with severe heat waves that are expected to occur in summer at the end of the century (Beniston, 2004), projected changes in heat wave attributes can yield a valuable spatial estimation of future heat-related risks on European societies.

#### 4.3. Changes in strong stress heat wave attributes

Figs. 8a, 9a and 10a depict spatial patterns of SHW frequencies, durations and amplitudes in summer for the present climate, respectively. We consider the following pairs of 20-year time-slices in order to explore future absolute changes in heat wave attributes: baseline (1990–2009) and, early 21st century (2015–2034), mid 21st century (2045–2064) and late 21st century (2075–2094). Since consistent spatial patterns are found among heat wave attributes, we mainly focus the discussion on amplitude for the sake of brevity. As aforementioned, HWA is the most relevant attribute for evaluating heat-related health risks. Note that amplitudes are normalized by the whole number of days for each considered period. In Europe, maximum amplitudes – up to 5 °C per heat wave day – are found in the southernmost parts of Spain, Greece and Turkey. Relatively high values – up to 1–2 °C per heat wave day – are located in Portugal, Italy, central Turkey, the most important southern European river basins and in some areas surrounding the Black Sea.

Projections suggest a steady increase and a northward expansion of SHW amplitudes. Important rises are expected for the Mediterranean European countries: southernmost Spain, Portugal, Italy, Greece and Turkey could increase SHW amplitudes to 5–7 °C per heat wave day by 2075–2094 (Fig. 10b–d). Main southern European river basins could suffer increases up to 4–5 °C per heat wave day. Accordingly, SHW frequencies and durations are also projected to drastically increase and further extend northwards. For the late century, SHW frequencies increase by 40–45 days per summer over large areas of the European Mediterranean countries. The transitional climate zone (TCZ) – between the Mediterranean to the south and the Baltic sea to the north – experience increases up to 20 days per summer (Fig. 8b–d). SHW durations could increase above 40 days per summer in southernmost Europe, and SHWs could last over 20 days more per summer in the European Mediterranean (Fig. 9b–d). Note that the ensemble-standard deviation increases along the century, a natural consequence of the increasing spread with time observed in multi-model climate scenarios and that the smallest ensemble-standard deviations are found where the ensemble-mean absolute changes are projected to be slighter.

The 21st century climate might bring the onset of non summery heat waves in parts of Europe. Analyzing the evolution of heat wave attributes in the transition seasons is an issue of maximum interest as many highly-dependent social and economic activities rely on the quality and length of climate seasonality. Van Ulden et al. (2007) have pointed out a projected trend towards more easterly circulation types over central Europe during summers which could imply higher temperatures, particularly in late summer. Fischer and Schär (2009) have indicated that a progressive European warming within the summer

might shift the timing of the maximum temperature of the seasonal cycle and favor heat waves to occur in early autumn by 2071–2100. More frequent strong stress heat waves in late spring and early summer or/and more frequent extreme stress heat waves could affect short-term acclimatization for humans. Nowadays, heat waves early in the summer have greater effects on heat-related morbidity and mortality than later in the same season. This is owed to the effect of short-term acclimatization to the thermal conditions through physiological and behavioral adaptation (Hajat et al., 2002).

In spring, the present spatial distribution does not depict remarkable SHW amplitudes over Europe. Projections point out only small changes throughout the twenty-first century: amplitudes could increase by 1 °C per heat wave day in the southernmost areas of Spain, Greece, Cyprus and Turkey by 2075–2094 (not shown). In autumn,

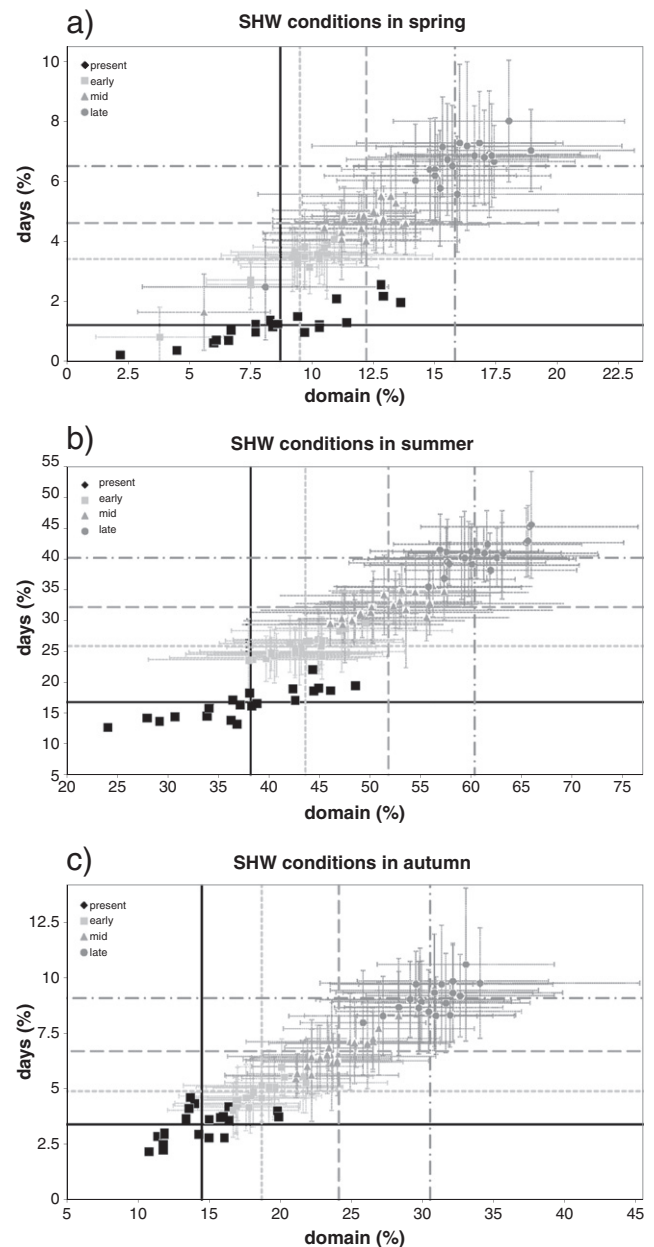


Fig. 11. Temporal and spatial coverage of SHW conditions for the present (1990–2009), early (2015–34), mid (2045–64) and late (2075–94) time-slices. Present coverage and projected ensemble-mean changes are shown for (a) spring, (b) summer and (c) autumn. Vertical and horizontal lines denote the multi-year means of temporal and spatial coverage for each time-slice. Also shown is the ensemble-standard deviation as thin dashed lines.

present SHW amplitudes exhibit values below 1 °C per heat wave day in the aforementioned regions. Projections indicate a noticeable increase for the European Mediterranean countries, as well as a northward incidence. Therefore, wide areas of southern Portugal, Spain, Italy, the Balkans and Turkey could suffer rises beyond 2 °C per day at the end of the century. The most important river basins in southern Europe may also experience increases above 1 °C per heat wave day (not shown).

General increases in SHW persistence and extent are expected for all seasons (Fig. 11). In spring and autumn, the most important rises could be mainly located over north Africa, doubling the present extent. Persistence is expected to treble in autumn and quadruple in spring. Therefore, persistence and extent increases are projected to occur at faster rates in transition seasons than in summer. Note that observations exhibit a greater inter-annual variability than projections, despite individual RCMs usually simulating increases in future climate variability. Projected inter-annual variability is highly smoothed in the ensemble-mean. Furthermore, ensemble-spread is higher for extent than for persistence.

#### 4.4. Changes in extreme stress heat wave attributes

Figs. 12a, 13a and 14a show the present spatial distribution of EHW attributes in summer. Again, consistent spatial patterns are found among EHW attributes throughout the century: steady increases and northward expansions are projected. The highest HWA in the present climate – up to 10 °C per heat wave day – are restricted to the south of the Atlas range in north Africa (Fig. 14a). Amplitudes up to 2 °C per heat wave day are found along the north African coastline, the lower Guadalquivir river basin, and in some scattered areas of the Turkish Mediterranean. By 2075–2094, projected extreme HWA increases range from 2 °C to 4 °C per heat wave day in southern Spain,

in some scattered areas of Mediterranean Italy, Greece and Turkey, and in Cyprus. The Italian peninsula, central Greece and Turkey, as well as the main southern European river basins might experience rises up to 2 °C per heat wave day (Fig. 14b–d). In addition, EHW frequencies are expected to dramatically increase in the European Mediterranean countries, with rises up to 40 days per summer at the end of the century (Fig. 12b–d). EHW durations are also expected to increase up to 25–30 days in these countries. Notable augmentations are projected around the Black Sea coast as well (Fig. 13b–d). Thus, extreme stress heat waves will become more severe, larger and longer lasting in south Europe and the Mediterranean.

In spring and autumn, EHW incidence is strictly confined to the south of the Atlas range. Projections do not indicate significant changes in the spatial attributes in Europe. By 2075–2094, only slight amplitude increases – below 1 °C per heat wave day – are projected in the southernmost parts of Spain, Italy, Greece, Cyprus and Turkey. On the contrary, EHW conditions might become more severe and extensive in North Africa (not shown). General increases in persistence and extent are expected for all seasons. Unlike SHWs, the rate of change is expected to be faster only for EHW persistence in the transition seasons. In summer, EHW persistence and extent are projected to double (Fig. 15). Note that present inter-annual variability exhibits the highest values in spring.

Strong and extreme stress heat wave spatial patterns are consistent with previous findings by Fischer and Schär (2010): the most severe heat-related risks on human health are projected to greatly increase in low-altitude regions – as coastal areas and lower river basins, whereas high-altitude areas could remain marginally affected. This fact is explained by the strong gradient with altitude and by the projected smaller reduction in daily minimum relative humidity along the coasts owing to the proximity to sea. Some authors have also indicated that an

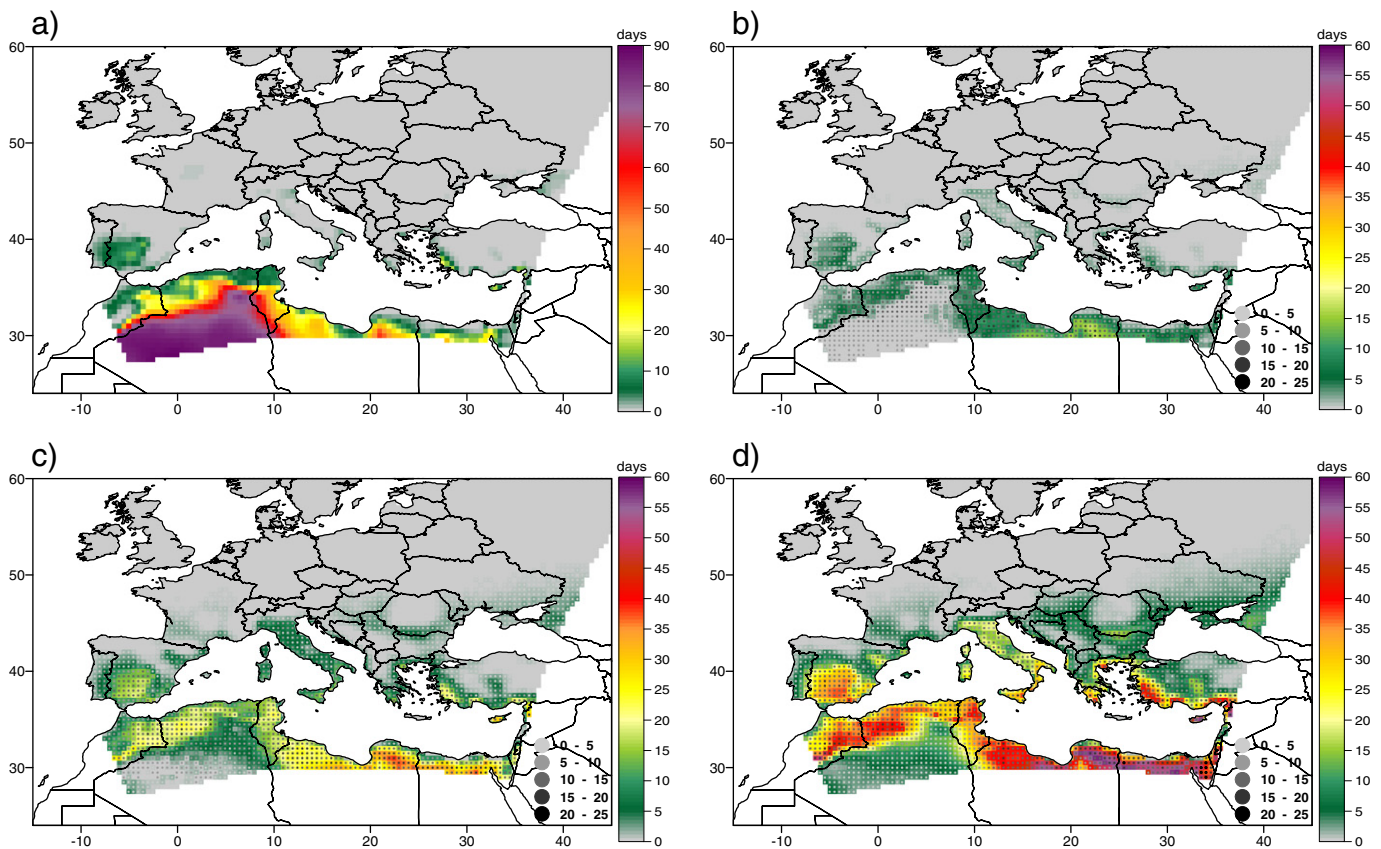


**Fig. 12.** Spatial distribution of (a) present (1990–2009) EHW frequency in summer; and projected ensemble-mean absolute changes for (b) early (2015–34), (c) mid (2045–64) and (d) late (2075–94) twenty-first century. Shaded circles show the ensemble-standard deviation according to the scale. Absolute changes and standard deviations are expressed as number of days.

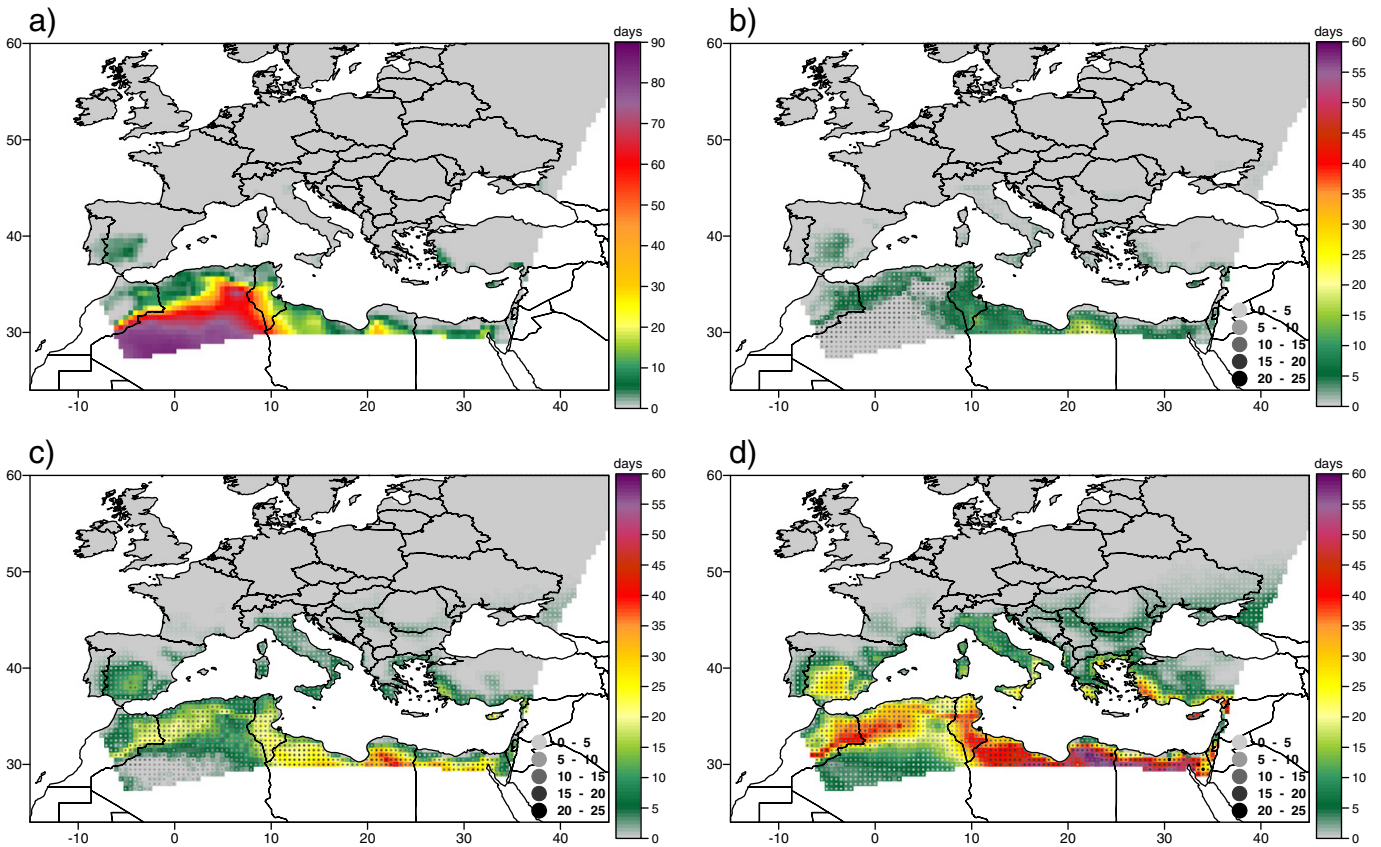


Fig. 13. As in Fig. 12, but for EHW duration.

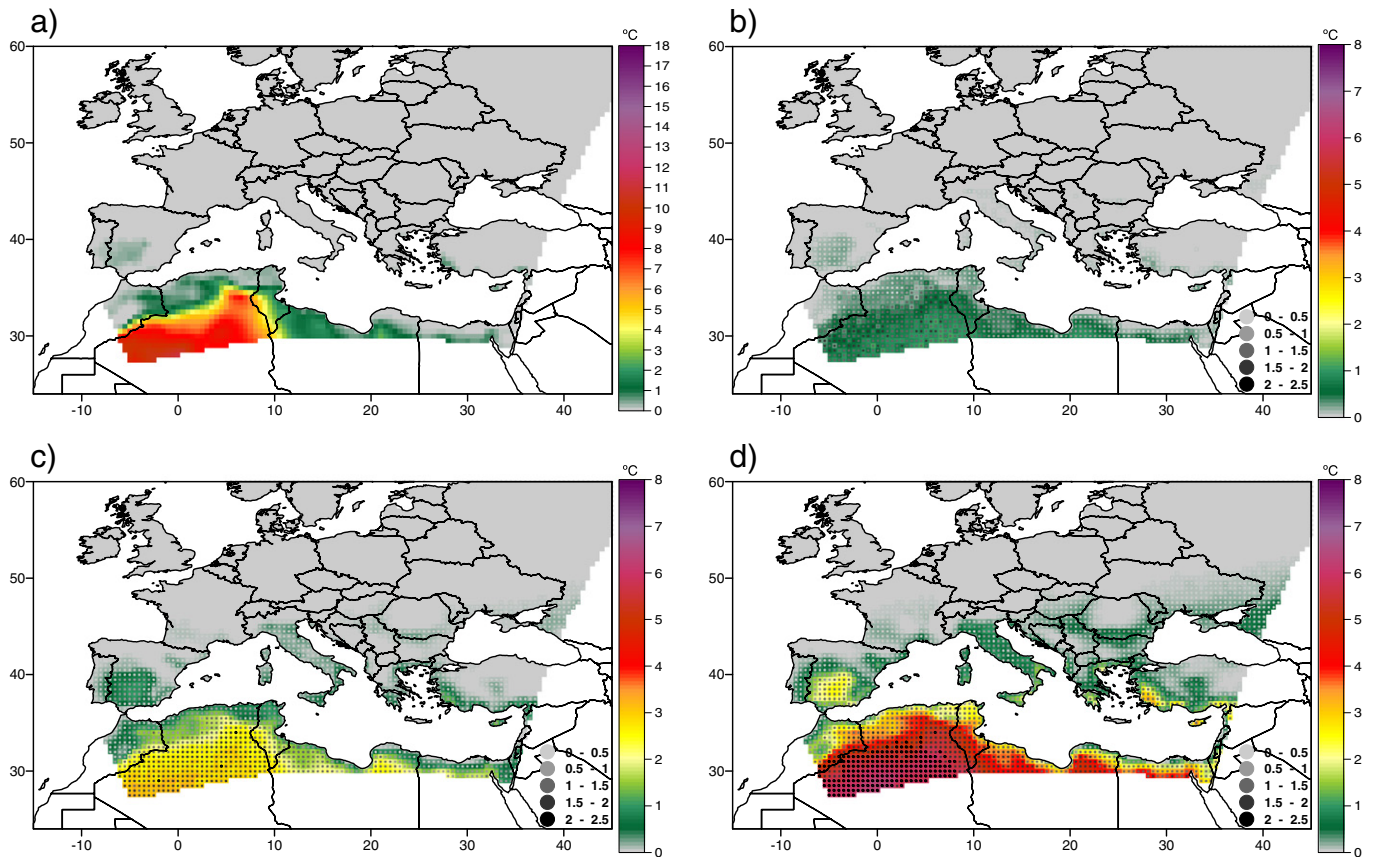


Fig. 14. As in Fig. 10, but for EHW amplitude.

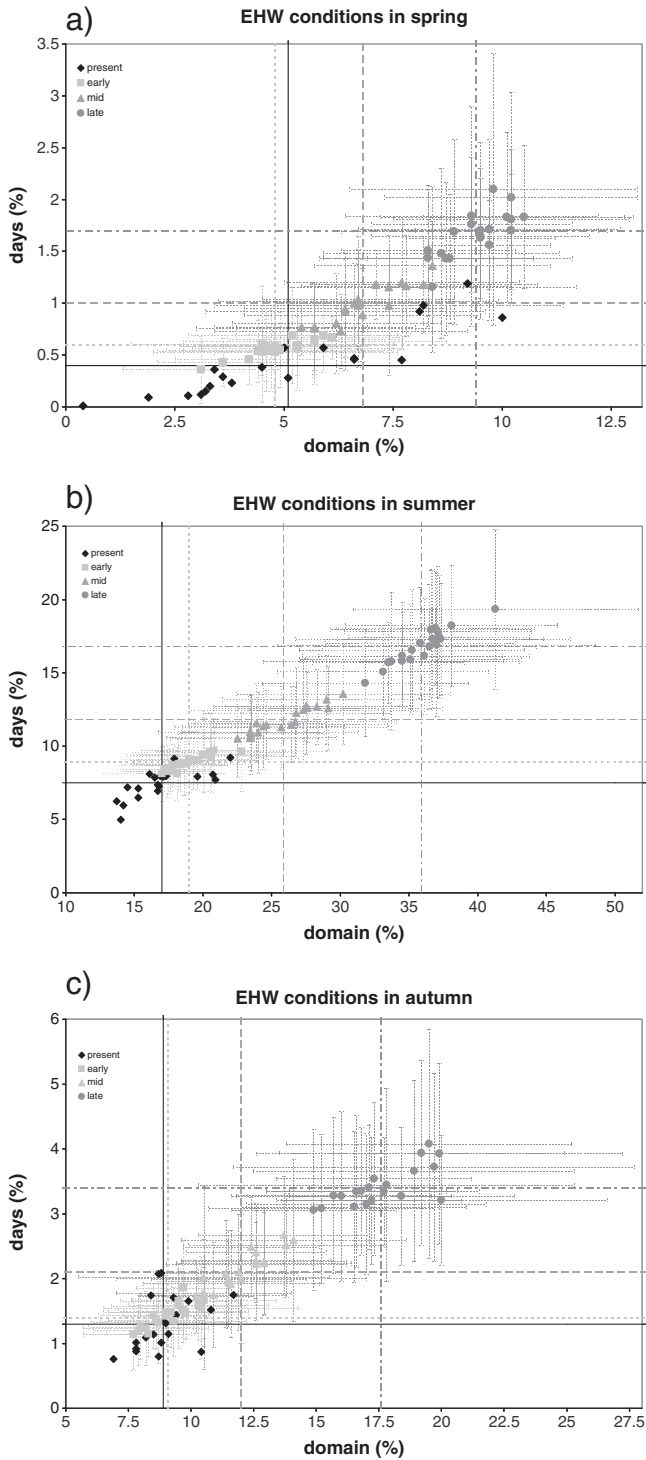


Fig. 15. As in Fig. 11, but for EHW conditions.

increase in the north–south pressure gradient across northern Europe could result in a reduction of windiness and cloudiness in the Mediterranean, thus providing indications of the physical mechanisms behind these results (Räsänen et al., 2004; Leckebusch et al., 2006).

### 5. Conclusions and further remarks

Heat waves significantly impact on human health, regional economies and the environment. Climate change will exacerbate the intensity of heat waves, becoming more severe. Furthermore, Europe arises as a

highly sensitive region to both the progressive summer warming and the changes in temperature variability. An assessment of present and future patterns of heat waves that highly impact human health in Europe has been carried out by using the thermo-physiological relevant PET index. Shifts in seasonality and changes in the rate of thermal stress have been evaluated as well. We have derived PETs from meteorological data coming from ERA-Interim reanalysis and a suite of regional climate models driven by the SRES A1B scenario. Next, we have applied a quantile–quantile adjustment to PETs derived from daily simulated atmospheric outputs in order to amend possible biases in the models. We have also adopted a multi-model ensemble approach to better encompass model and boundary condition uncertainties. The application of all these approaches results in a more reliable assessment of possible future changes of heat waves leading to high impacts on human health over Europe.

Two kinds of high-impact heat waves have been defined depending on intensity and then characterized by means of a set of heat wave attributes. Amplitude is the most appropriate indicator to both evaluate our heat wave definitions and assess heat-related risks on human health. Heat wave amplitude integrates thermal stress exceedance over the entire period under heat wave conditions. Accordingly, we have correlated spatial patterns of strong and extreme stress heat wave amplitudes with mortality excess during the summer of 2003 in Europe. Even if a straightforward relationship between acute thermal stress and duration thresholds and heat-related mortality excess is elusive, we have found relatively strong positive spatial correlations.

Therefore, results yield a valuable estimation of those European regions more vulnerable in the coming decades to heat-related impacts on human health. Although an explicit inference of projected mortality excess under future strong and extreme stress heat wave conditions in Europe is out of the scope of this work, it arises as a valuable subject for further research. The unequivocal signal detected in our results towards more frequent and more intense heat waves in Europe provides the foundation for an extension of this work towards further investigations using a comprehensive and multidisciplinary methodology. From social scientists and public health managers to architects and urban planners shall contribute to the precise description of the heat-related impacts over human beings and society. In this context, the UTCI index (further information on the special issue of *Int. J. Biometeorol.*, 56, 2012), as the current international standard based on recent scientific progress in thermo-physiological modeling of the human response to environmental conditions, shall be used. It is worth also noting that it has been only possible to test the link between heat wave amplitudes and mortality excess for the 2003 heat wave, since no more mortality databases are available for other similar events over Europe. When larger mortality databases will be available for other hazardous heat waves, future research will allow to further assess the link between heat wave amplitudes and mortality excess by considering a wider climatology.

Consistent steady increases and northward advances in the incidence of strong and extreme stress heat wave attributes are projected for Europe throughout this century. The largest changes are expected to occur in southern Europe and the Mediterranean. This region is densely populated – currently by more than 400 million people, and climate change will pose enhanced heat-induced health risks to their inhabitants. Heat wave impacts are particularly harmful for the most vulnerable groups of society living in urban areas, owing to the amplifying effects of the urban heat island and pollution. However, heat wave impacts on humans strongly rely on personal, demographic and regional factors as well. For instance, a decline is found when examining the evolution of heat related mortality in the United States due to the increased use of air conditioning. Therefore, changes in vulnerability and the role of political decision making are essential facets. Mitigation strategies could substantially reduce the effects of a future increase in severity for European heat waves. Awareness campaigns, early heat warning systems, housing and building acclimatization, or action plans addressed to deprived people can be achieved by implementing

the appropriate policies. In fact, many European countries have already implemented comprehensive action protocols after the unprecedented 2003 summer heat wave (Lowe et al., 2011). Ultimately, climate projections for Europe reveal that the population will be exposed to higher health risks related with heat waves that demand action from the administrations and civil protection bodies.

## Acknowledgments

Two anonymous reviewers are acknowledged for their valuable comments which helped to improve the quality of this manuscript. Drs. Jean-Marie Robine and François Richard Herrmann are deeply acknowledged for providing mortality data. Prof. Andreas Matzarakis is also acknowledged for providing the RayMan-Pro model. The scientific results and conclusions, as well as any views or opinions expressed herein, are those of the author(s) and do not necessarily reflect the views of NOAA or the Department of Commerce. This work has been partially sponsored by the CGL2008-01271/CLI (MEDICANES) and CGL2011-24458 (PREDIMED) projects from the Spanish Ministerio de Ciencia e Innovación; and by ESTCENA project (200800050084078), a strategic action from Plan Nacional de I+D+i 2008–11 funded by Ministerio de Medio Ambiente y Medio Rural y Marino. The authors also acknowledge the ENSEMBLES project, funded by the European Commission's 6th Framework Programme, through contract GOCE-CT-2003-505539.

## References

- Akima, H., 1978. A method of bivariate interpolation and smooth surface fitting for irregularly distributed data points. *ACM Trans. Math. Softw.* 4, 148–164.
- Akima, H., 1996. Algorithm 761: scattered-data surface fitting that has the accuracy of a cubic polynomial. *ACM Trans. Math. Softw.* 22, 362–371.
- Amengual, A., Homar, V., Romero, R., Alonso, S., Ramis, C., 2012. A statistical adjustment of regional climate model outputs to local scales: application to Platja de Palma, Spain. *J. Clim.* 25 (3), 939–957.
- ASHRAE, 2004. Thermal Environmental Conditions for Human Occupancy. ASHRAE Standard 55-2004. ASHARE Inc., Atlanta, GA, USA.
- Ballester, J., Robine, J.M., Herrmann, F.R., Rodó, X., 2011. Long-term projections and acclimatization scenarios of temperature-related mortality in Europe. *Nat. Commun.* 2, 358.
- Basu, R., Samet, J.M., 2002. Relation between elevated ambient temperature and mortality: a review of the epidemiologic evidence. *Epidemiol. Rev.* 24 (2), 190–202.
- Beniston, M., 2004. The 2003 heat wave in Europe: a shape of things to come? An analysis based on Swiss climatological data and model simulations. *Geophys. Res. Lett.* 41, L02202.
- Beniston, M., et al., 2007. Future extreme events in European climate: an exploration of regional climate model projections. *Clim. Chang.* 81, 71–95.
- Blazejczyk, K., Epstein, Y., Jendritzky, G., Staiger, H., Tinz, B., 2012. Comparison of UTCI to selected thermal indices. *Int. J. Biometeorol.* 56 (3), 515–535.
- Boé, J., Terray, L., Habets, F., Martin, E., 2007. Statistical and dynamical downscaling of the Seine basin climate for hydro-meteorological studies. *Int. J. Climatol.* 27, 1643–1655.
- Bolton, D., 1980. The computation of equivalent potential temperature. *Mon. Weather Rev.* 108, 1046–1053.
- Bröde, P., Fiala, D., Blazejczyk, K., Holmér, I., Jendritzky, G., Kampmann, B., Tinz, B., Havenith, G., 2012. Deriving the operational procedure for the Universal Thermal Climate Index (UTCI). *Int. J. Biometeorol.* 56 (3), 481–494.
- Changnon, S.A., Kunkel, K.E., Reinke, B.C., 1996. Impacts and responses to the 1995 heat wave: a call to action. *Bull. Am. Meteorol. Soc.* 77, 1497–1506.
- Dee, D.P., et al., 2011. The ERA-Interim reanalysis: configuration and performance of the data assimilation system. *Q. J. R. Meteorol. Soc.* 137, 553–597.
- Déqué, M., 2007. Frequency of precipitation and temperature extremes over France in an anthropogenic scenario: model results and statistical correction according to observed values. *Glob. Planet. Chang.* 57, 16–26.
- Fanger, P.O., 1972. *Thermal Comfort*. McGraw Hill, New York.
- Fanger, P.O., Højbjerg, J., Thomsen, J.O.B., 1974. Thermal comfort conditions in the morning and in the evening. *Int. J. Biometeorol.* 18, 1622.
- Fink, A.H., Brücher, T., Krüger, A., Leckebusch, G.C., Pinto, J.G., Ulbrich, U., 2004. The 2003 European summer heatwaves and drought – synoptic diagnosis and impacts. *Weather* 59, 209–216.
- Fischer, E.M., Schär, C., 2009. Future changes in daily summer temperature variability: driving processes and role for temperature extremes. *Clim. Dyn.* 33, 917–935.
- Fischer, E.M., Schär, C., 2010. Consistent geographical patterns of changes in high-impact European heat waves. *Nat. Geosci.* 3, 398–403.
- Giorgi, F., 2004. Climate change hot-spots. *Geophys. Res. Lett.* 33, L08707.
- Hajat, S., Kovats, R.S., Atkinson, R.W., Haines, A., 2002. Impact of hot temperatures on death in London: a time series approach. *J. Epidemiol. Community Health* 56 (5), 367–372.
- Hewitt, C.D., Griggs, D.J., 2004. Ensembles-based predictions of climate changes and their impacts. *EOS Trans. Am. Geophys. Union* 85, 566.
- Ho, C.K., Stephenson, D.B., Collins, M., Ferro, C.A.T., Brown, S.J., 2012. Calibration strategies: a source of additional uncertainty in climate change projections. *Bull. Am. Meteorol. Soc.* 93, 21–26.
- Höppe, P., 1999. The physiological equivalent temperature – a universal index for the biometeorological assessment of the thermal environment. *Int. J. Biometeorol.* 43 (2), 71–75.
- IPCC, 2007. Climate change 2007: the physical science basis. In: Solomon, S., Qin, D., Manning, M., Chen, Z., Marquis, M., Averyt, K.B., Tignor, M., Miller, H.L. (Eds.), Contribution of Working Group I to the Fourth Assessment Report of the Intergovernmental Panel on Climate Change. Cambridge University Press, Cambridge, United Kingdom and New York, NY, USA.
- Jendritzky, G., Tinz, B., 2009. The thermal environment of the human being on the global scale. *Glob. Health Action* 2. <http://dx.doi.org/10.3402/gha.v2i0.2005>.
- Kjellström, E., Bärning, L., Jacob, D., Jones, R., Lenderink, G., Schär, C., 2007. Modelling daily temperature extremes: recent climate and future changes over Europe. *Clim. Chang.* 81, 249–265.
- Koppe, C., Kovats, S., Jendritzky, G., Menne, B., Breuer, D.J., 2004. Heat Waves: Risks and Responses. Regional Office for Europe, World Health Organization.
- Leckebusch, G.C., et al., 2006. Analysis of frequency and intensity of winter storm events in Europe on synoptic and regional scales from a multi-model perspective. *Clim. Res.* 31, 59–74.
- Lowe, D., Ebi, K.L., Forsberg, B., 2011. Heatwave early warning systems and adaptation advice to reduce human health consequences of heatwaves. *Int. J. Environ. Res. Public Health* 8, 4623–4648. <http://dx.doi.org/10.3390/ijerph8124623>.
- Matzarakis, A., Amelung, B., 2008. Physiological equivalent temperature as indicator for impacts of climate change on thermal comfort of humans. Seasonal forecasts, climatic change and human health. *Adv. Glob. Chang. Res.* 30, 161–172.
- Matzarakis, A., Mayer, H., 1997. Heat stress in Greece. *Int. J. Biometeorol.* 41 (1), 34–39.
- Matzarakis, A., Nastos, P.T., 2011. Human-biometeorological assessment of heat waves in Athens. *Theor. Appl. Climatol.* 105, 99–106.
- Matzarakis, A., Mayer, H., Iziomon, M.G., 1999. Applications of a universal thermal index: physiological equivalent temperature. *Int. J. Biometeorol.* 43 (2), 76–84.
- Matzarakis, A., Rutz, F., Mayer, H., 2007. Modelling radiation fluxes in simple and complex environments – application of the RayMan model. *Int. J. Biometeorol.* 51, 323–334.
- Matzarakis, A., Rutz, F., Mayer, H., 2010. Modelling radiation fluxes in simple and complex environments: basics of the RayMan model. *Int. J. Biometeorol.* 54, 131–139.
- Matzarakis, A., Muthers, S., Koch, E., 2011. Human biometeorological evaluation of heat-related mortality in Vienna. *Theor. Appl. Climatol.* 105, 1–10.
- Mayer, H., Höppe, P., 1987. Thermal comfort of man in different urban environments. *Theor. Appl. Climatol.* 38 (1), 43–49.
- Meehl, G.A., Tebaldi, C., 2004. More intense, more frequent, and longer lasting heat waves in the 21st century. *Science* 305, 994–997.
- Muthers, S., Matzarakis, A., Koch, E., 2010. Climate change and mortality in Vienna—a human biometeorological analysis based on regional climate modeling. *Int. J. Environ. Res. Public Health* 7, 2965–2977.
- Nakicenovic, N., et al., 2000. Emissions scenarios. A Special Report of Working Group III of the Intergovernmental Panel on Climate Change. Cambridge University Press, Cambridge, UK and New York, NY, p. 599.
- Nastos, P.T., Matzarakis, A., 2012. The effect of air temperature and human thermal indices on mortality in Athens, Greece. *Theor. Appl. Climatol.* 108, 591–599.
- Räisänen, J., et al., 2004. European climate in the late 21st century: regional simulations with two driving global models and two forcing scenarios. *Clim. Dyn.* 22, 13–31.
- Reichle, R.H., Koster, R.D., 2004. Bias reduction in short records of satellite soil moisture. *Geophys. Res. Lett.* 31, L19501. <http://dx.doi.org/10.1029/2004GL020938>.
- Robine, J.M., Cheung, S.L.K., Le Roy, S., Van Oyen, H., Griffiths, C., Michel, J.P., Herrmann, F.R., 2008. Death toll exceeded 70,000 in Europe during the summer of 2003. *C. R. Biologies* 331, 171–178.
- Robinson, P.J., 2001. On the definition of a heat wave. *J. Appl. Meteorol.* 40, 762–765.
- Schär, C., Jendritzky, G., 2004. Hot news from summer 2003. *Nature* 432, 559–560.
- Schär, C., Vidale, P.L., Lüthi, D., Frei, C., Häbert, C., Liniger, M., Appenzeller, C., 2004. The role of increasing temperature variability in European summer heatwaves. *Nature* 332–336.
- Trigo, R.M., Ramos, A., Nogueira, P., Santos, F.D., García-Herrera, R., Gouveia, C., Santo, F.E., 2009. Evaluating the impact of extreme temperature based indices in 2003 heat wave excessive mortality in Portugal. *Environ. Sci. Policy* 12, 844–854.
- Van Ulden, A., Lenderink, G., van den Hurk, B., van Meijgaard, E., 2007. Circulation statistics and climate change in central Europe: PRUDENCE simulations and observations. *Clim. Chang.* 81, 179–192.
- Wood, A., Leung, L.R., Sridhar, V., Lettenmaier, D.P., 2004. Hydrologic implications of dynamical and statistical approaches to downscaling climate outputs. *Clim. Chang.* 62, 189–216.